ACS APPLIED MATERIALS & INTERFACES

Research Article

www.acsami.org

Clickable Multifunctional Dumbbell Particles for in Situ Multiplex Single-Cell Cytokine Detection

Peng Zhao,[†] Justin George,[†] Bin Li,[†] Nooshin Amini,[#] Janet Paluh,[#] and Jun Wang*[,†,‡]

[†]Multiplex Biotechnology Laboratory, Department of Chemistry, University at Albany, State University of New York, Albany, New York 12222, United States

[#]College of Nanoscale Science and Engineering, State University of New York Polytechnic Institute, Albany, New York 12203, United States

[‡]Cancer Research Center, University at Albany, State University of New York, Rensselaer, New York 12144, United States

Supporting Information

ABSTRACT: We report a novel strategy for fabrication of multifunctional dumbbell particles (DPs) through click chemistry for monitoring single-cell cytokine releasing. Two different types of DPs were prepared on a large scale through covalent bioorthogonal reaction between methyltetrazine and trans-cyclooctene on a microchip under a magnetic field. After collection of the DPs, the two sides of each particle were further functionalized with different antibodies for cell capturing and cytokine detection, respectively. These DPs labeled with different fluorescent dyes have been used for multiplex detection and analysis of cytokines secreted by single live cells. Our results show that this new type of DPs are promising for applications in cell sorting, bioimaging, single-cell analysis, and biomedical diagnostics.

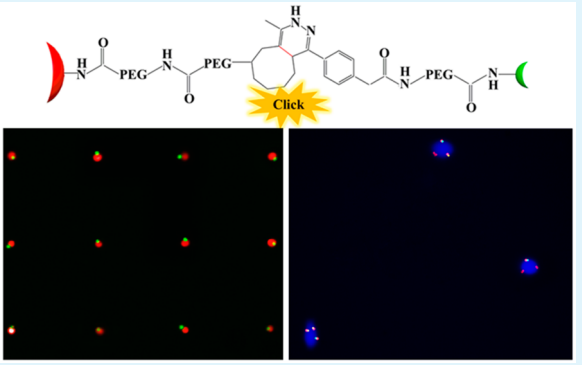

KEYWORDS: *microspheres, dumbbell, microarray, single cell, cytokine*

1. INTRODUCTION

Janus particles possessing distinct surfaces with different chemical compositions have attracted enormous attention.[1] The asymmetry of the surfaces drastically imparts the particles directionality and new physical/chemical properties, such as optical activity, mechanical strength, and electronic and magnetic properties, which are inconceivable for homogeneous symmetric particles. The compartmentalization of Janus particles is highly dependent on synthesis approaches, which are normally based on modification of immobilized particles on a surface, microfluidic solidification, and phase separation.[2−5] Although a variety of Janus particles have been introduced in the past decade, exploration of their biomedical applications has only been emerging recently.[6,7]

The major challenge that hinders the adoption of Janus particles in biomedical applications is the lack of easy-to-follow strategy for generating the nano- to micro-sized anisotropic particles, which possess practically useful functionalities superior to their homogeneous counterparts.[8] For example, the phase separation synthesis methods rely on the interaction energy between precursors and therefore require special fabrication conditions.[9,10] Surface immobilization approaches often result in limited quantities of produced particles that are not enough for molecular and cellular analyses. This is mainly because a high quality of monolayer must be ensured but adversely is difficult to scale up.[11] Other synthesis methods such as microfluidic techniques, seed polymerization technology, and gel trapping,[10−12] are either not amenable to scale up or not convenient for further functionalization and applications.

The other related issue about the utility of Janus particle is to find a niche where the special functionality of the particles converges with real biomedical needs. Thus, the chemical composition of the particles should be tailored to biomolecule conjugation. Conjugation of antiepidermal growth factor receptor antibody on one side of dumbbell shape Au−Fe_3O_4 nanoparticles (NPs) facilitates the engulfment of particles while the Au compartment enables optical visualization of cancer cells.[13] The similar strategy has been used for multimodal dark-field, surface-enhanced Raman spectroscopy, two-photon and fluorescence imaging as well as MRI imaging.[14,15] Many complicated Janus particles have been used as barcoding device for multiplexed sensing of DNA and proteins.[16−18] These conjugations have not been integrated into fabrication process, or are not as convenient as click chemistry. The bioorthogonal reaction between a tetrazine (Tz) and a trans-cyclooctene (TCO) has been used for small molecular labeling.[19] The [4 + 2] cycloaddition is fast, chemoselective, and does not require a catalyst. This clickable reaction permits conjugation of virtually

Received: June 10, 2017
Accepted: September 8, 2017
Published: September 8, 2017

DOI: 10.1021/acsami.7b08338
ACS Appl. Mater. Interfaces XXXX, XXX, XXX−XXX

all kinds of proteins and oligonucleotides with a support substrate.

Techniques at the micro scale are ideal for single-cell analysis because of comparable size. However, Janus microparticles have not been applied for single-cell analysis yet, to the best of our knowledge. Single cells, particularly immune cells, are intrinsically heterogeneous to carry out their necessary biological functions. For instance, macrophages secrete large amount of inflammatory factors such as tumor necrosis factor α (TNFα) to fight invasion of bacteria and viruses. Conventional approach for single-cell cytokine detection is primarily enzyme-linked immunospot.[20] Flow cytometry can also measure cytokines by blocking protein transporter on membrane, which would inevitably influence other signaling pathways of the cell.[21] Microfluidics-based methods allow for quantification of tens of cytokines in single cells.[22] However, the microchip operation procedure is intimidating to many biomedical users, and those microchips are not well commercialized yet. Currently, there is still a lack of user-friendly technique for single-cell cytokine detection without special instruments.

In this work, we present a unique microarray-assisted approach for large-scale fabrication of dumbbell particles (DPs) via Tz and TCO click reaction, with a demonstrated application in continuous detection of cytokine TNFα secretion by single live macrophage cells. Big magnetic microspheres (bMS, 2.7 μm) carrying TCO are anchored to microwells of a microarray first, and another magnetic microspheres of various sizes carrying Tz then attach vertically to the bMS through Tz-TCO click reaction to form dumbbells. After linking bMS and sMS with different types of oligonucleotides through click reaction, prepared DPs are collected using PMMA membrane as a sacrifice layer. Through DNA hybridization between oligonucleotides on the microparticles and their complementary oligonucleotides that are conjugated with antibodies, sMS are covered with anti-CD14 antibody for cell attachment, and bMS are coated with anti-TNFα antibody for in situ TNFα capture over time. With periodical sandwich enzyme-linked immunosorbent assay (ELISA) detection, we have observed increase of TNFα signal and vast heterogeneity between single cells in response to lipopolysaccharide (LPS) stimulation. Likewise, multiplex detection of cytokine is achieved using different dye and antibodies. Our approach has potential for point-of-detection single-cell cytokine analysis of tissue samples without single cell isolation and breakup of intercellular connectivity.

2. MATERIALS AND METHODS

2.1. Materials. Dynabeads MyOne Silane (1 μm), Dynabeads amine (2.7 μm), 3-aminopropyltriethoxysilane (APTES), Hoechst 33342, CellTracker Blue CMAC Dye, and Streptavidin-Alexa 647 (SA-Alexa 647) were obtained from Thermo Fisher Scientific; 200 nm magnetic amine NPs were obtained from Ocean Nanotech (San Diego). FMOC-NH-PEG-SC (Mw 10 000) was purchased from Laysan Bio. Inc. Trans-cyclooctene-PEG_{12}-NHS ester (TCO-NHS) and Methyltetrazine-Sulfo-NHS ester (Tz-NHS) were obtained from Click Chemistry Tools Company. Cyanine2-NHS, Cyanine3-NHS and Cyanine5-NHS were purchased from Lumiprobe. TNFα, mouse interferon γ (IFNγ), mouse IL-10, antimouse TNFα monoclonal antibody, antimouse IFNγ monoclonal antibody, antimouse IL-10 monoclonal antibody, biotin antimouse TNFα polyclonal antibody, biotin antimouse IFNγ polyclonal antibody, biotin antimouse IL-10 polyclonal antibody, rat antimouse CD14 monoclonal antibody, and Alexa 488-antirat IgG were purchased from Biolegend. Succinimidyl-4-formylbenzoate (S-4FB) and succinimidyl-6-hydrazinonicotinamide (S-HyNic) were purchased from Solulink. Aqueous solutions were prepared using Milli-Q (MQ) water. Phosphate-buffered saline (PBS) used in this work contains 137 mM NaCl, 2.7 mM KCl, 8 mM Na_2HPO_4, and 2 mM KH_2PO_4 at pH 7.4.

2.2. Microwell Chip Fabrication. The poly(dimethylsiloxane) (PDMS) microwell chip was fabricated using standard microfabrication soft-lithographic technique. A master for PDMS molding was obtained by patterning photoresist SU-8 2005 at a depth of 5 μm on a silicon wafer. The PDMS prepolymer (Sylgard 184, Dow Corning) was mixed in a ratio of 10:1, and subsequently casted on the lithographically patterned replication. After curing at 70 °C for 2 h, the PDMS replica was separated from the master.

The master for the other half of the PDMS chip was based on a cut tape attached on a silicon wafer. The depth was measured to be about 100 μm. This PDMS replica was aligned with the microwell PDMS to form a microchip with a wide microfluidic channel.

2.3. Preparation of TCO-bMS and Tz-sMS. One hundred microliters of 30 mg mL^{-1} amine-bMS were washed with MQ for 3 times, and mixed with 1 mg of FMOC-NH-PEG-SC for 4 h. The microspheres were washed for 3 times to remove unreacted PEG. FMOC was deprotected by incubating the modified microspheres with 50% piperidine in dichloromethane for 10 min. The exposed amine was reacted with 1 μL of 0.2 mg mL^{-1} NHS-TCO solution for another 4 h. At last, the TCO coated bMS were washed and collected using a magnet, and were stored at 4 °C for further use. Likewise, bMS-Tz were prepared using the same procedure.

The sMS bought from the vendor have silane group on the surface. One hundred microliters of 40 mg mL^{-1} sMS were washed with MQ for 3 times, and were then mixed with 200 μL of APTES in 10 mL of anhydrous acetone at room temperature for 10 min. The microspheres were washed and resuspended in 100 μL of PBS, and were mixed with 1 mg of FMOC-NH-PEG-SC at room temperature for 4 h before washing for 3 times. FMOC was deprotected by the same method above. The modified microsphere were further reacted with 1 μL of 0.2 mg mL^{-1} NHS-Tz solution for another 4 h. At last, the Tz-sMS was washed and collected using a magnet. They were stored at 4 °C for further use.

2.4. Fabrication of DPs. 200 nm magnetic NPs were drop coated onto the surface of array after plasma treatment for 60 s, and were baked at 100 °C for 10 min. The NPs outside of microwells were removed using a scotch tape. The microwell PDMS was baked on a hot plate at 150 °C for 2 h so the NPs strongly stick to each other and the wells. After the microchip was cooled to room temperature, the microwell PDMS was attached to another PDMS to form a microchannel. Fifty microliters of 4 μg mL^{-1} NHS-Tz solution was added into the microchip chamber from the inlet and incubated for 1 h. Residual NHS-Tz was removed by washing for 3 times.

50 μL of 0.2 mg mL^{-1} TCO-bMS solution was added to microchip channel from the inlet where the microchip was placed within a copper wired coil. An external magnetic field (about 100 mT) was immediately turned on. After 30 min, the magnetic field was turned off, and the microchip was washed to remove extra TCO-bMS with MQ water for 3 times. Almost all TCO-bMS outside of microwells can be washed away.

The same procedure described above for TCO-bMS was used for Tz-sMS patterning in the microchip.

2.5. Collection and Functionalization of DPs. Two types of amine-modified oligonucleotides, labeled as D and E, were used to modify the surface of DPs. One microliter of 0.2 mg mL^{-1} NHS-TCO and NHS-Tz was mixed with 100 μL of 0.2 mM oligonucleotide D and E for 4 h, respectively, followed with Zeba desalting columns purification and stored at 4 °C for further use.

Fifty microliters of 0.2 mM Tz-E conjugates were carefully flowed from the microchip inlet and reacted with TCO-bMS for 30 min. After 3 times washing with PBS, 50 μL of 0.2 mM TCO−D conjugates were flowed from the microchip inlet and reacted for 30 min, followed by another 3 times washing.

To release dumbbells, PMMA anisole solution (5%) was drop coated on the microwells, followed by heating on a hot plate at 50 °C for 10 min to evaporate anisole and solidify PMMA. The PMMA

DOI: 10.1021/acsami.7b08338
ACS Appl. Mater. Interfaces XXXX, XXX, XXX−XXX

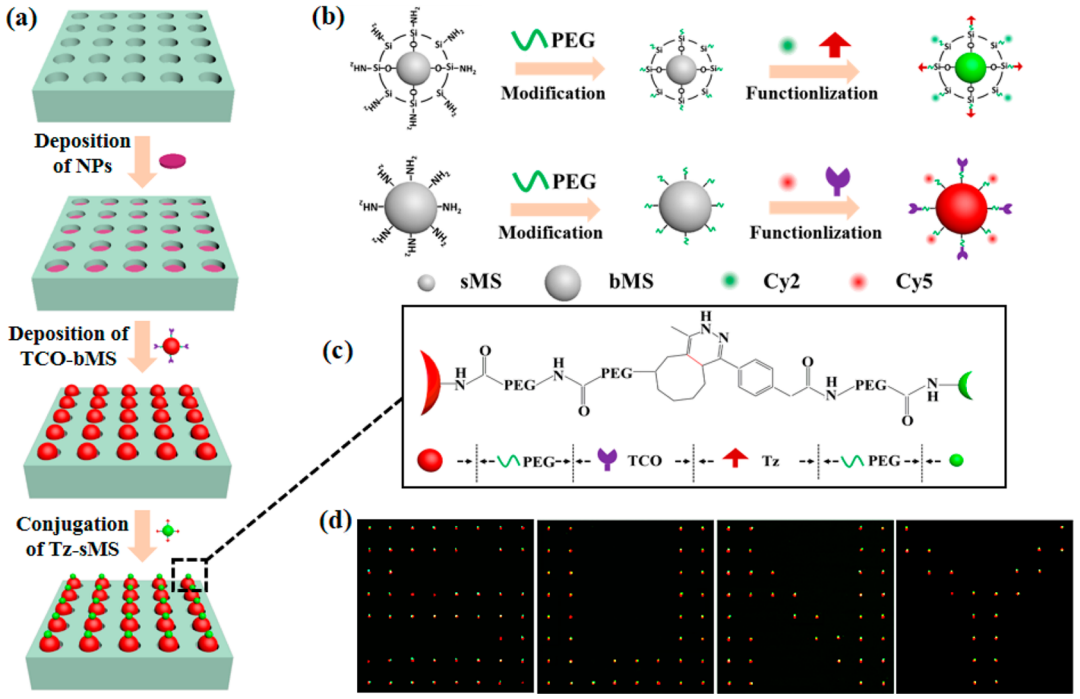

Figure 1. (a) General scheme for fabrication of DPs. The microwells of a PDMS replica are filled with 200 nm magnetic NPs first. They are functionalized with Tz for tethering TCO-bMS (red). The latter is further conjugated with Tz-sMS (green). The deposition of TCO-bMS and conjugation of Tz-sMS is performed under a magnetic field to ensure only one microsphere on a microwell for each time. (b) Surface functionalization of bMS and sMS. Long chain PEG is linked on the surface on one end and is functionalized with Tz/Cy2 or TCO/Cy5 on the other end. (c) Schematic structure of linkage between TCO-bMS and Tz-sMS. (d) Overlap of fluorescence images of bMS and sMS on microwells, with a pattern of "S", "U", "N", and "Y". Most microwells show yellow color, indicating the presence of both bMS and sMS.

membrane was manually peeled off and transferred to a Petri dish, and then was immersed into glacial acetic acid for overnight to dissolve the PMMA. Particles were washed and collected using a magnet.

After collection, the sMS of DPs were further functionalized with anti-CD14 antibody through hybridization between oligonucleotide D on the microparticle surface and the complementary D′ on anti-CD14 antibody. The same procedure was followed for bMS functionalization with anti-TNFα antibody using oligonucleotide E-complementary oligonucleotide E′ hybridization. Conjugation of D′ with anti-CD14 antibody and E′ with anti-TNFα antibody were performed using S-4FB and S-HyNic linkers. In the first step, the amine of D′ and E′ was converted to 4-formylbenzamide group, and the amine on the antibodies was converted to 6-hydrazinonicotinamide. The formation of the Schiff base by reaction of 4-FB and 6-hydrazinonicotinamide at pH 6.0 coupled the antibodies to oligos, resulting in D′-anti-CD14 antibody (100 μM) and E′-anti-TNFα antibody (100 μM). For functionalization, 10 μL of 10 μg mL^{-1} DPs were mixed with a cocktail of 20 μL D′-anti-CD14 antibody conjugates at 100 μM and E′-anti-TNFα antibody conjugates at 100 μM for 1 h, followed by 3 times washing with PBST (0.1% Tween 20 in PBS).

2.6. Cell Culture and Cytokine Detection. The macrophage cell line Raw 264.7 was purchased from American Type Culture Collection, and were routinely cultured in a T25 cm^2 flask containing Dulbecco's modified Eagle's medium/F12 (DMEM/F12) supplemented with 10% FBS, 100 U mL^{-1} of penicillin, and 0.1 mg mL^{-1} of streptomycin. All cultures were incubated at 37 °C under 5% CO_2 atmosphere.

For calibration of the ELISA assay, recombinant mouse TNFα was serially diluted to various concentrations ranging between 10 pg mL^{-1} and 5 ng mL^{-1} in PBST. Briefly, 10 μL of 10 μg mL^{-1} antibodies conjugated DPs were incubated with 40 μL of TNFα with various concentrations in 1% BSA/PBS at room temperature for 2 h. Biotinylated anti-TNFα detection antibody was preincubated with Streptavidin-Alexa 647 with a molar ratio 1:3. After 3 times washing of residual TNFα recombinant protein, the detection antibody conglomerate at a concentration of 10 nM was then added to the DPs, and was incubated for 1 h. The DPs were washed with PBST for 3 times before imaging.

For in situ cytokine detection, macrophages were stimulated with 1 μg mL^{-1} LPS in complete culture medium and labeled with 1 μg mL^{-1} CellTracker Blue dye, and were immediately seeded into a 96 well plate at 1 × 10^4 cell/well. 1 × 10^4 DPs conjugated with both anti-CD14 antibody and anti-TNFα antibody were added to cells. The same ELISA detection strategy aforementioned above was used to detect the secreted TNFα by live cells at the incubation time of 0, 3, 6, 9, 12, and 24 h, where only culture medium was used to 1% BSA/PBS. Only single cells attached with one DP were imaged, and the fluorescence intensity was recorded.

Likewise, the other two dye and antibodies were linked and performed using the same approach.

2.7. Microscopy Imaging. Images of the chip and cells after staining were taken systematically on an inverted fluorescence microscope (Olympus IX73) equipped with three fluorescent filter sets: a green fluorescein filter set (U-FF, Olympus; excitation filter 450−490 nm, dichroic 500 nm long pass, emission 520 nm long pass), a yellow Cy3 filter set (U-FF, Olympus; excitation filter 528−553 nm dichroic 565 nm long pass, emission 590−650 nm), and a red Cy5 filter set (U-FF, Olympus; excitation filter 590−650 nm, dichroic 660 nm long pass, emission 665−740 nm). A microscope objective (UPlanApo, Olympus, 4X/0.16; UPlanFLN, Olympus, 10X/0.30/Ph1; UCPlanFLN, Olympus, 20X/0.70/Ph2) was used to collect fluorescence light. A digital camera (Zyla sCMOS, Andor) mounted on the microscope was used to capture images using Andor SOLIS software. Scanning electron microscope (SEM) images were taken by using a LEO (Zeiss) 1550 microscopy.

3. RESULTS AND DISCUSSION

The general procedure of fabricating dumbbell shape microparticle pairs is illustrated in Figure 1a. We first filled the microwells of a PDMS replica with 200 nm amine functionalized magnetic NPs. After baking, a layer of magnetic NPs with

DOI: 10.1021/acsami.7b08338
ACS Appl. Mater. Interfaces XXXX, XXX, XXX−XXX

the depth of ~3.5 μm was formed on the bottom of each microwell across the whole chip. These NP pallets in microwells serve as the base for anchoring bMS and consecutively sMS to form DPs. The amine group was then conjugated with Tz. bMS tagged with PEG_{10000}-TCO and sMS tagged with PEG_{10000}-Tz were added onto the microwells sequentially under a magnetic field. With a strong external magnetic field at 100 mT, the induced magnetism on the 200 nm nanoparticle pallet of each well forces bMS or sMS to form a vertical chain above (Video S1). After removal of the external magnetic field, the relaxation of superparamagnetism results in separation of microspheres except those anchored through Tz-TCO click reaction. We have optimized the concentration of microspheres for loading into the microchip chamber with ~100 μm depth, in order to ensure only one microsphere at one time on each microwell and obtain a high yield (Figures S1 and S2). A concentration greater than 1×10^7 particles mL^{-1} would lead to more than one microsphere rail on each array spot, while a concentration less than 1×10^5 particles mL^{-1} would results in no rails on many array spots and thereafter low fabrication efficiency. Because long chain PEG was used to coat the microsphere surface, < 5% nonspecific binding (two or more identical beads together) was observed. The final step is to transfer DPs from the microwells with PMMA and release them in a solution.

The key to formation of DPs is chemical modification of their surface. We linked long chain PEG_{10000} on both bMS and sMS so that each pair is semiflexible and stabilized to lower the influence of shear force in between. PEG_{500} was also tested, which resulted in much lower yield after collection, most likely because the linkage was too short and stiff. Other linking strategies by oligonucleotide paring and streptavidin−biotin interaction have shown a yield <10%. That is because those binding forces are still far lower than covalent chemical bond. Interestingly, we show that the size of DPs is changeable, as the conjugation between bMS and bMS can also form dumbbells (Figure S3). However, the yield is relatively lower than that of DPs between bMS and sMS, maybe because the shear force within two bMS is much higher under the same experimental condition.

After deprotection of FMOC group on the other end of PEG on microspheres, amine group is activated and ready to react with bioorthogonal linker Tz/TCO succinimidyl ester (Figure 1b, c). Tz/TCO click chemistry was chosen not only because they react extremely fast, but also because it provides a platform widely open for conjugation with other biomolecules. As a proof of concept, the bMS and sMS were coupled covalently with TCO and Cy5 dye at a ratio of 100:1 and with Tz and Cy2 also at a ratio of 100:1, respectively. Thus, the majority of TCO and Tz on surface is still available for further conjugation. With the current surface modification design, the yield of the first layer of bMS reaches ~90% over 10,000 microwells, and <5% particles reside outside of microwells. The second layer of sMS has a yield of ~70%. Repeating the same procedure by loading the same microspheres and washing for a few cycles can further increase the yield.

Figure 2a shows the dumbbells on the microwells before releasing. Although only a trivial portion of amine groups was modified with Cy5 (red) and Cy2 (green) dyes, the labeling was good enough for visualization. The fluorescence changes of bMS (red channel) clearly shows the binding of bMS. Overlapping the red and green channels indicates specific coupling of the microspheres. A microarray with letters "S", "U", "N" and "Y" (abbreviation for "State University of New York") was designed for patterning DPs. As shown in Figure 1d, the bMS and sMS are well overlapped and are deposited only in the designated microwells.

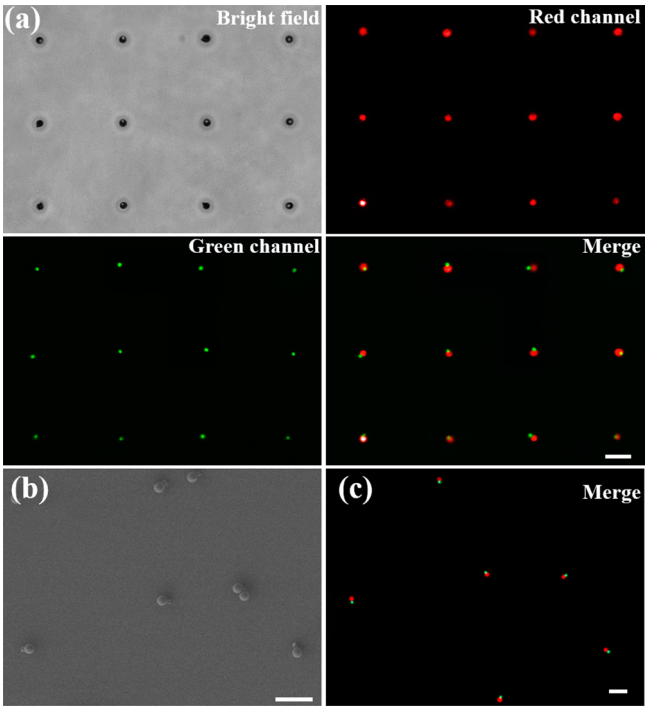

Figure 2. (a) Bright-field and fluorescence images of the DPs on chip. (b) SEM image of DPs. (c) Merged fluorescence image of DPs after release from the microchip and collection. All scale bar: 10 μm.

Before detachment of DPs from microwells, the remaining Tz and TCO on the particle surface were reacted with TCO-oligonucleotide and Tz-oligonucleotide, respectively. Oligo DNAs can survive mildly harsh environment and mostly keep intact. PMMA was used as a sacrifice layer to lift DPs and resuspend them in another solution. The validity of the collection was confirmed by SEM images and fluorescence images (Figure 2b, c and Figure S4b, c). We can see that most of the DPs were successfully collected, with a few trimers and single microspheres.

The utility of the DPs in cell attachment and single-cell cytokine detection was investigated. Macrophage cells were used because they produce large amount of TNFα upon stimulation by LPS and the secretion is heterogeneous between cells.[23] Just like other macrophages, Raw 264.7 cells highly express CD14 on their surface (Figure S5).[24] The oligonucleotide on sMS was hybridized with its complementary single stranded oligo DNA that is conjugated with anti-CD14 antibody. So the sMS can specifically bind to cells through antibody−antigen interaction (Figure 3). This binding lasts >24 h and endures multiple cycles of washing. By contrast, DPs without anti-CD14 modification barely bind to cells (Figure 3b).

When anti-CD14 antibody and anti-TNFα antibody were anchored on sMS and bMS of each DP, the bMS side was employed to detect secretion of TNFα over time through sandwich ELISA (Figure 4a).[25] We first calibrate the detection system using recombinant proteins to quantitate the detection limit. Figure 4b shows the fluorescence intensity of bMS at various concentration of recombinant TNFα ranging from 10

DOI: 10.1021/acsami.7b08338
ACS Appl. Mater. Interfaces XXXX, XXX, XXX−XXX

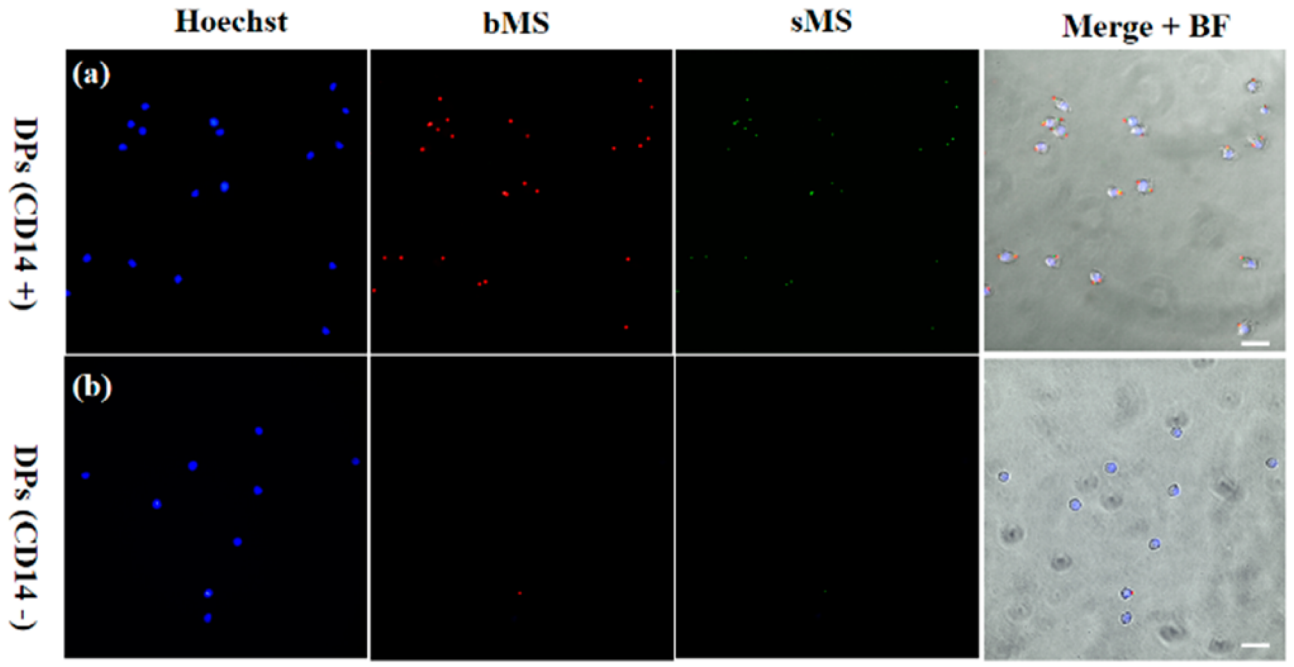

Figure 3. Images of DPs (a) coated with anti-CD14 antibody and (b) without anti-CD14 antibody on macrophage cells that are stained with Hoechst 33342. Scale bar: 20 μm.

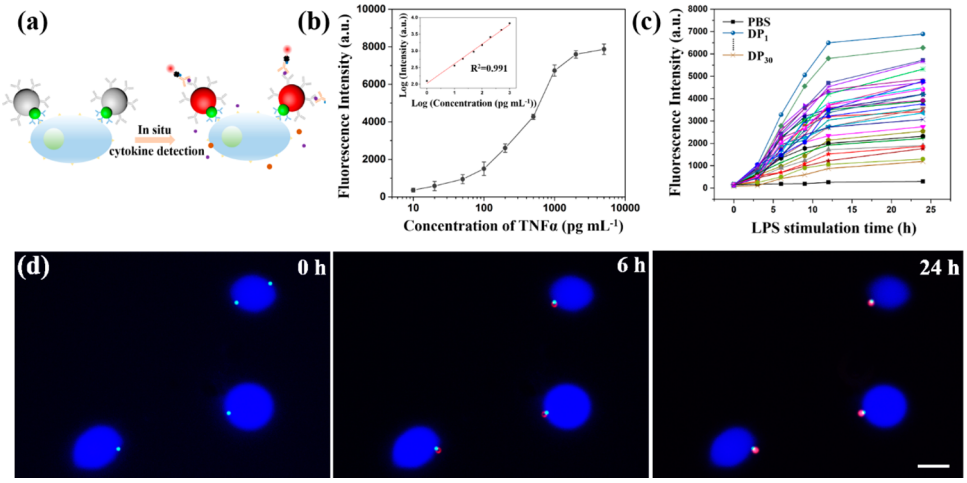

Figure 4. (a) Schematic illustration of attachment of DPs to single cells and in situ sandwich ELISA detection of cytokine released by the cells. (b) Calibration curve of recombinant TNFα concentration vs fluorescence intensity of detection DPs. Inset Figure with logarithm axes shows linear relationship. (c) Continuous detection of TNFα of single cells at the LPS stimulation time of 0, 3, 6, 9, 12, and 24 h. The fluorescence intensities of 30 DPs (labeled as DP_1, DP_2... DP_{30}) on 30 different single cells are recorded. PBS means control experiment without LPS stimulation. (d) Merged fluorescence images of cell (blue) and DPs (green, sMS; red, bMS) after ELISA detection. The images were taken at 0, 6, and 24 h LPS stimulation time. Cells were stained with CellTracker Blue CMAC dye. Scale bar: 10 μm.

pg mL^{-1} to 5 ng mL^{-1}. The detection limit was determined at 16 pg mL^{-1}, which is comparable to that by standard well plate based-ELISA. This result indicates that there is sufficient antibody coating on the microsphere's surface. We have also quantitated the coating variations between the DPs. The measured variation of fluorescence is measured below 5% across 500 DPs.

Next, we demonstrate the continuous single-cell detection of TNFα secretion using the DPs. In this in situ cytokine detection, the sMS was used not only to attach cells but also to indicate the presence of a DP, which is further validated by bright-field images. After attachment of DPs to cells, LPS at 1 μg mL^{-1} was added to the culture medium and CellTracker Blue dye was used to label live macrophages. The proinflammatory cytokines such as TNFα and IFNγ are produced upon stimulation by LPS through toll-like receptor 4 pathway, while the anti-inflammatory cytokine IL-10 could be generated simultaneously.[26,27] They are preferentially captured by the antibodies on the DPs in the close vicinity. Therefore, we hypothesize that periodically detected proteins on the DPs reflect the cytokine secretion kinetics. We only chose the cells with a separation distance at least 20 μm for the single-cell cytokine detection, in order to minimize the influence of signal from the neighboring cells. We periodically replaced culture medium with a staining solution comprised of biotinylated anti-TNFα detection antibody and Alexa 647-streptavidin, and

DOI: 10.1021/acsami.7b08338
ACS Appl. Mater. Interfaces XXXX, XXX, XXX−XXX

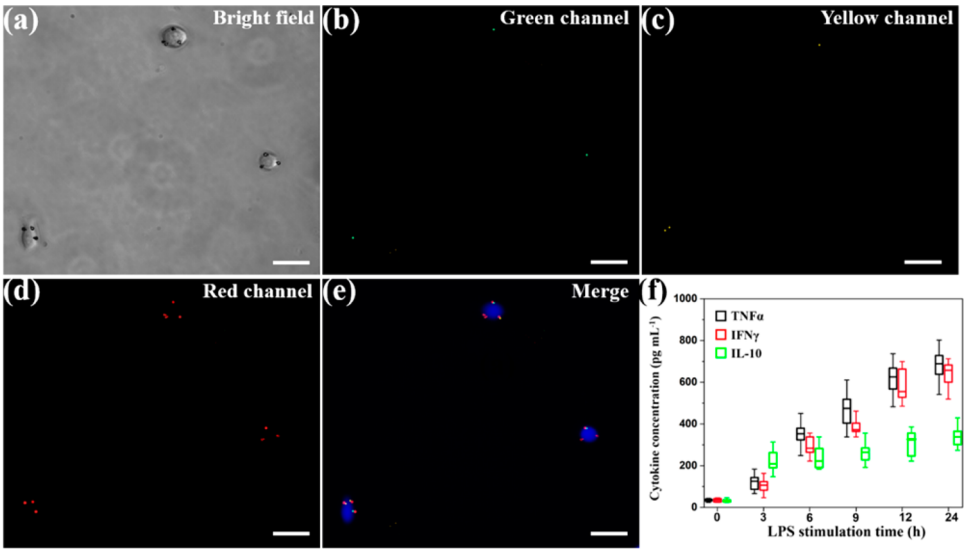

Figure 5. (a) Bright-field image of three DPs attaching to cells. (b–d) Fluorescent images of three different channels for DPs after ELISA detection. (e) Merged fluorescence image of cells (blue) and three different DPs. The images were taken at 24 h LPS stimulation time. Cells were stained with CellTracker Blue CMAC dye. (f) Box plot of TNFα, IFNγ, and IL-10 secretion levels by macrophage cells after LPS stimulation for 24 h. Whiskers calculated adopting the Tukey method. Outliers not shown. All scale bar: 20 μm.

incubated them with DPs for 1 h each time. This fast ELISA effectively reduces the impact of detection procedure on cells' physiological activities. Figure 4c shows the fluorescence intensities of bMS of DPs from 30 individual cells. Cells show various responses to the same stimulation, as the TNFα releasing amount and rate are dramatically different between cells. In comparison, no signal was detected without LPS stimulation. Because the measure error of DPs is less than 5%, the observed dramatic variation is believed to attribute to the biological heterogeneity. Figure 4d shows fluorescence images taken at 0, 6, and 24 h after LPS injection. These pictures permit visualization of the fluorescence intensity changes of bMS, suggesting the successful attachment to cell surface as well as in situ detection of cytokine secreted by living cells.

At last, multiplex detection of cytokine from cells with different stimulation durations has been performed using DPs with different dyes and antibodies. Both dye (Cy2, Cy3 or Cy5) and anti-CD14 antibody were anchored on sMS, respectively, while anti-TNFα antibody, anti-IFNγ antibody or anti-IL-10 antibody was linked to corresponding bMS of each DP. The DPs were attached to individual cells, and ELISA detection was conducted periodically. The fluorescence intensity of DPs was quantitated at each time point, for DPs modified with Cy5, only the fluorescence of bMS which were not affected by sMS were quantitated. Figure 5a shows the bright-field image of DPs attached to the surface of cells. Figure 5e is a merged sample image of multiplex cytokine detection after LPS stimulation for 24 h. sMS show different fluorescent colors (Figure 5b–d), indicating the tagging of different fluorophores. Different fluorescence intensities were also observed on the bMS because proteins were variably secreted and subsequently detected (Figure 5d). As shown in Figure 5f (134 cells for each data point), activated macrophage cells produce significant amounts of TNFα and IFNγ but less IL-10. IL-10 was barely secreted after LPS stimulating for 3 h. Our result is consistent with the expectation, because IL-10 is known to counter-regulate and inhibit immune system activation and proliferation by suppressing the expression of pro-inflammatory cotokines, such as IL-2, IL-5, TNFα and IFNγ.[28,29]

4. CONCLUSION

In conclusion, we introduce a novel method to fabricate multifunctional DPs with two different sizes on a large scale via Tz-TCO click chemistry. The dumbbells were formed on a microarray first and were subsequently released and resuspended in an aqueous solution. The two sides of each dumbbell were linked with two different antibodies for cell attachment as wells as cytokine detection. In situ detection of TNFα was achieved by linking DPs to the surface of macrophage cells using anti-CD14 antibody. With sufficient detection sensitivity, we have quantitated the secretion kinetics of individual cells over 24 h. We also demonstrated multiplex detection of three different cytokines for individual macrophage cells. The current method presents the first step toward construction of more complex anisotropic particles. Our analytical approach is potentially applicable for cell sorting and simultaneously multiplex cytokine detection on a variety of cell types at the single-cell level.

■ ASSOCIATED CONTENT

Supporting Information

The Supporting Information is available free of charge on the ACS Publications website at DOI: 10.1021/acsami.7b08338.

Additional experimental results of fabrication and detection (PDF)

Video S1 (AVI)

■ AUTHOR INFORMATION

Corresponding Author

*E-mail: jwang34@albany.edu.

ORCID

Jun Wang: 0000-0002-8781-8248

Author Contributions

The manuscript was written through contributions of all authors. All authors have given approval to the final version of the manuscript.

DOI: 10.1021/acsami.7b08338
ACS Appl. Mater. Interfaces XXXX, XXX, XXX–XXX

Funding

This work was supported by the Presidential Initiatives Fund for Research and Scholarship, and startup fund by SUNY Albany to J.W.

Notes

The authors declare no competing financial interest.

■ ACKNOWLEDGMENTS

We thank Dr. Max Royzen from the Department of Chemistry for helpful discussion and constructive advice of click chemistry.

■ REFERENCES

(1) Kim, J. W.; Lee, D.; Shum, H. C.; Weitz, D. A. Colloid Surfactants for Emulsion Stabilization. *Adv. Mater.* **2008**, *20*, 3239−3243.
(2) Liang, F.; Zhang, C.; Yang, Z. Rational Design and Synthesis of Janus Composites. *Adv. Mater.* **2014**, *26*, 6944−6949.
(3) Prevo, B. G.; Velev, O. D. Controlled, Rapid Deposition of Structured Coating from Micro- and Nanoparticle Suspensions. *Langmuir* **2004**, *20*, 2099−2107.
(4) Erb, R. M.; Jenness, N. J.; Clark, R. L.; Yellen, B. B. Towards Holonomic Control of Janus Particles in Optomagnetic Traps. *Adv. Mater.* **2009**, *21*, 4825−4829.
(5) Lin, W. F.; Swartz, L. A.; Li, J. R.; Liu, Y.; Liu, G. Y. Particle Lithography Enables Fabrication of Multicomponent Nanostructures. *J. Phys. Chem. C* **2013**, *117*, 23279−23285.
(6) Yang, S.; Guo, F.; Kiraly, B.; Mao, X.; Lu, M.; Leong, K. W.; Huang, T. J. Microfluidic Synthesis of Multifunctional Janus Particles for Biomedical Applications. *Lab Chip* **2012**, *12*, 2097−2102.
(7) Zhao, Y.; Cheng, Y.; Shang, L.; Wang, J.; Xie, Z.; Gu, Z. Microfluidic Synthesis of Barcode Particles for Multiplex Assays. *Small* **2015**, *11*, 151−174.
(8) Yi, Y.; Sanchez, L.; Gao, Y.; Yu, Y. Janus Particles for Biological Imaging and Sensing. *Analyst* **2016**, *141*, 3526−3539.
(9) Wang, X.; Feng, X.; Ma, G.; Yao, L.; Ge, M. Amphiphilic Janus Particles Generated via a Combination of Diffusion-Induced Phase Separation and Magnetically Driven Dewetting and Their Synergistic Self-Assembly. *Adv. Mater.* **2016**, *28*, 3131−3137.
(10) Kim, J. W.; Cho, J.; Cho, J.; Park, B. J.; Kim, Y. J.; Choi, K. H.; Kim, J. W. Synthesis of Monodisperse Bi-Compartmentalized Amphiphilic Janus Microparticles for Tailored Assembly at the Oil-Water Interface. *Angew. Chem., Int. Ed.* **2016**, *55*, 4509−4513.
(11) Feng, L.; Dreyfus, R.; Sha, R.; Seeman, N. C.; Chaikin, P. M. DNA Patch Particles. *Adv. Mater.* **2013**, *25*, 2779−2783.
(12) Nie, L.; Liu, S.; Shen, W.; Chen, D.; Jiang, M. One-pot Synthesis of Amphiphilic Polymeric Janus Particles and Their Self-Assembly into Supermicelles with a Narrow Size Distribution. *Angew. Chem., Int. Ed.* **2007**, *46*, 6321−6324.
(13) Xu, C.; Xie, J.; Ho, D.; Wang, C.; Kohler, N.; Walsh, E. G.; Morgan, J. R.; Chin, Y. E.; Sun, S. Au-Fe_3O_4 Dumbbell Nanoparticles as Dual-functional Probes. *Angew. Chem., Int. Ed.* **2008**, *47*, 173−176.
(14) Wu, L. Y.; Ross, B. M.; Hong, S.; Lee, L. P. Bioinspired Nanocorals with Decoupled Cellular Targeting and Sensing Functionality. *Small* **2010**, *6*, 503−507.
(15) Schick, I.; Lorenz, S.; Gehrig, D.; Schilmann, A. M.; Bauer, H.; Panthofer, M.; Fischer, K.; Strand, D.; Laquai, F.; Tremel, W. Multifunctional Two-photon Active Silica-Coated Au@MnO Janus Particles for Selective Dual Functionalization and Imaging. *J. Am. Chem. Soc.* **2014**, *136*, 2473−2483.
(16) Nicewarner-Pena, S. R.; Freeman, R. G.; Reiss, B. D.; He, L.; Pena, D. J.; Walton, I. D.; Cromer, R.; Keating, C. D.; Natan, M. J. Submicrometer Metallic Barcodes. *Science* **2001**, *294*, 137−141.
(17) Pregibon, D. C.; Toner, M.; Doyle, P. S. Multifunctional Encoded Particles for High-Throughput Biomolecule Analysis. *Science* **2007**, *315*, 1393−1396.
(18) Lee, J.; Bisso, P. W.; Srinivas, R. L.; Kim, J. J.; Swiston, A. J.; Doyle, P. S. Universal Process-Inert Encoding Architecture for Polymer Microparticles. *Nat. Mater.* **2014**, *13*, 524−529.
(19) Karver, M. R.; Weissleder, R.; Hilderbrand, S. A. Bioorthogonal Reaction Paris Enable Simultaneous, Selective, Multi-Target Imaging. *Angew. Chem., Int. Ed.* **2012**, *51*, 920−922.
(20) Czerkinsky, C. C.; Nilsson, L. A.; Nygren, H.; Ouchterlony, O.; Tarkowski, A. A Solid-Phase Enzyme-Linked Immunospot (ELI-SPOT) Assay for Enumeration of Specific Antibody-Secreting cells. *J. Immunol. Methods* **1983**, *65*, 109−121.
(21) Wang, J.; Tham, D.; Wei, W.; Shin, Y. S.; Ma, C.; Ahmad, H.; Shi, Q. H.; Yu, J. K.; Levine, R. D.; Heath, J. R. Quantitating Cell-Cell Interaction Functions with Applications to Glioblastoma Multiforme Cancer Cells. *Nano Lett.* **2012**, *12*, 6101−6106.
(22) Lu, Y.; Xue, Q.; Eisele, M. R.; Sulistijo, E. S.; Brower, K.; Han, L.; Amir, E. D.; Pe'er, D.; Miller-Jensen, K.; Fan, R. Highly Multiplexed Profiling of Single-Cell Effector Functions Reveals Deep Functional Heterogeneity in Response to Pathogenic Ligands. *Proc. Natl. Acad. Sci. U. S. A.* **2015**, *112*, E607−E615.
(23) George, J. V.; Wang, J. Assay of Genome-Wide Transcriptome and Secreted Proteins on the Same Single Immune Cells by Microfluidics and RNA Sequencing. *Anal. Chem.* **2016**, *88*, 10309−10315.
(24) Lichtman, S. N.; Wang, J.; Lemasters, J. J. LPS Receptor CD14 Participates in Release of TNF-Alpha in RAW 264.7 and Peritoneal Cells but not in Kupffer Cells. *Am. J. Physiol.* **1998**, *275*, G39−G46.
(25) Zhao, P.; Wu, Y.; Zhu, Y.; Yang, X.; Jiang, X.; Xiao, J.; Zhang, Y.; Li, C. Upconversion Fluorescent Strip Sensor for Rapid Determination of Vibrio Anguillarum. *Nanoscale* **2014**, *6*, 3804−3809.
(26) Murray, P. J. The Primary Mechanism of the IL-10-Regulated Antiinflammatory Response is to Selectively Inhibit Transcription. *Proc. Natl. Acad. Sci. U. S. A.* **2005**, *102*, 8686−8691.
(27) Couper, K. N.; Blount, D. G.; Riley, E. M. IL-10: the Master Regulator of Immunity to Infection. *J. Immunol.* **2008**, *180*, 5771−5777.
(28) Taga, K.; Tosato, G. IL-10 Inhibits Human T Cell Proliferation and IL-2 Production. *J. Immunol.* **1992**, *148*, 1143−1148.
(29) Oh, B.; Chen, P.; Nidetz, R.; McHugh, W.; Fu, J.; Shanley, T. P.; Cornell, T. T.; Kurabayashi, K. Multiplexed Nanoplasmonic Temporal of T-Cell Response under Immunomodulatory Agent Exposure. *ACS Sens.* **2016**, *1*, 941−948.

DOI: 10.1021/acsami.7b08338
ACS Appl. Mater. Interfaces XXXX, XXX, XXX−XXX